

Theory of Casimir Forces without the Proximity-Force Approximation

Luciano C. Lapas,¹ Agustín Pérez-Madrid,² and J. Miguel Rubí²

¹*Interdisciplinary Center for Natural Sciences, UNILA, P.O. Box 2067, 85867-970 Foz do Iguaçu, Brazil*

²*Departament de Física Fonamental, Facultat de Física, Universitat de Barcelona, Avinguda Diagonal 647, 08028 Barcelona, Spain*

(Received 4 November 2015; published 18 March 2016)

We analyze both the attractive and repulsive Casimir-Lifshitz forces recently reported in experimental investigations. By using a kinetic approach, we obtain the Casimir forces from the power absorbed by the materials. We consider collective material excitations through a set of relaxation times distributed in frequency according to a log-normal function. A generalized expression for these forces for arbitrary values of temperature is obtained. We compare our results with experimental measurements and conclude that the model goes beyond the proximity-force approximation.

DOI: 10.1103/PhysRevLett.116.110601

Introduction.—The existence of attractive forces between two closely separated perfectly conducting plates due to quantum vacuum electromagnetic fluctuations was predicted by Casimir [1] and extended by Lifshitz [2], taking into account dielectric media. The first accurate experimental confirmation of the Casimir effect was reported in Refs. [3,4] and compared with the prediction by the proximity-force approximation (PFA) [5,6], which is supposedly valid when the characteristic curvature radii of the objects are large in relation to their intersurface separation [7]. Recent advances in nanotechnology making experimental measurements more accessible and accurate [8] have promoted a renewed interest in the Casimir effect and its dependence on the geometry of the device and the properties of the constituent material. The Casimir-Lifshitz forces have become a classical topic in quantum field theory, condensed matter physics, nano-optics, and atomic physics, also acting upon the correct functioning of micro-electromechanical systems [9]. At small separations, repulsive Casimir-Lifshitz forces have been discussed and measurements have been reported [10–12].

Much of the theoretical analysis of Casimir forces is based on the PFA. Some discrepancies between theoretical and experimental results have been reported and attributed to various origins [13,14], including temperature and dissipation effects [15] providing corrections beyond the PFA. Obtaining accurate expressions for the Casimir-Lifshitz force could be relevant in the design of devices at the nano- or microscale.

In this Letter, we present an analysis based on a kinetic model that paves the way to explain the Casimir-Lifshitz forces measurements beyond the PFA. We address the problem of deviations from the PFA in the study of complex relaxation processes, thus avoiding the approximation in terms of the curvature of materials. In addition, Casimir forces are calculated without referring to zero-point energies, relativistic van der Waals forces, and coupled ground-state energy; a comprehensive review

can be found in Ref. [16]. We verify our theory using recent experimental results reported in Refs. [10,13].

Proximity-force approximation.—Since the seminal work of Derjaguin [5], the PFA has been widely used to describe forces between perfectly conducting oppositely curved bodies in terms of the interaction between two parallel plates. According to the PFA, the Casimir-Lifshitz forces between a sphere of radius R and a plate separated by a distance $d \ll R$ can be written as

$$F_{\text{PFA}} = 2\pi R \varepsilon^{p-p}, \quad (1)$$

where ε^{p-p} is the separation-dependent interaction energy per unit area between two parallel plates composed of the same materials as the sphere-plate system. For perfectly conducting smooth parallel plates, $\varepsilon^{p-p} = -\pi^2 \hbar c / (720 d^3)$, where \hbar is the reduced Planck constant and c is the speed of light. Since the main deviations from the PFA arise from curvature, depending only on the geometrical ratio d/R , one can expand the curvature effects of the exact Casimir-Lifshitz force in powers of d/R as [7,13,17]

$$F_{\text{PFA}} = \alpha \frac{2\pi^3 R \hbar c}{720 d^3} \left[1 + \beta \frac{d}{R} + \mathcal{O}\left(\frac{d^2}{R^2}\right) \right], \quad (2)$$

where α and β are the correction coefficients to the PFA; e.g., $\alpha = 1$ for real scalar-field fluctuation, $\alpha = 2$ for an electromagnetic field, and $\beta = -0.564$ for perfect reflectors at $T = 0$ as well as at room temperature for short separation [14,18]. In this approach, higher order corrections to the PFA are neglected.

Kinetic model.—In the model we propose, the power absorbed by the hot material, $\dot{Q}_1(\omega)$, maintained at temperature T_1 , must be proportional to the energy current $J_{2 \rightarrow 1}(\omega, T_2)$ radiated by the cold material at temperature T_2 ,

$$\dot{Q}_1(\omega) = a_1(\omega, T_1, T_2) J_{2 \rightarrow 1}(\omega, T_2), \quad (3)$$

where $a_1(\omega, T_1, T_2)$ is the absorption coefficient, which may, in general, depend on the temperature of both surfaces. Likewise, the energy flow radiated by a particular material must be proportional to the rate of change of the energy of the corresponding radiation field,

$$J_{2 \rightarrow 1}(\omega, T_2) = e_2(\omega, T_2) \dot{u}(\omega, T_2), \quad (4)$$

where $e_2(\omega, T_2)$ is the emission coefficient. Here, the crucial point is the rate of change of the energy \dot{u} of the radiation field. Prior to the calculation of \dot{u} , some considerations must be given. To begin with, we can think that the dynamics of the system, constituted by photon gas and materials, arise upon adding collective excitations or modes of vibration of very diverse origin. Consequently, in the stationary state the energy of the system results from the superposition of the energies of these modes. Each of these modes reaches a stationary state in its own time scale. According to the Matthiessen rule, an overall relaxation time τ can be defined through $\tau^{-1} = \tau_1^{-1} + \dots + \tau_n^{-1}$, where all the τ_i correspond to independent scattering events [19]. In addition, let us assume that the decay of collective excitations takes place by a concatenation of cascade processes such that $\tau_\ell^{-1} = \tau_{\ell-1}^{-1} + \xi_\ell \tau_{\ell-1}^{-1}$, where ξ_ℓ represents a small random elementary input. Thus, one can derive $\tau_\ell^{-1} = \tau_0^{-1} (1 + \sum_{i=1}^{\ell} \xi_i)$, valid up to the first order. For large ℓ , $\sum \xi_i$ is asymptotically normally distributed, leading to [20]

$$\tau^{-1}(\omega) = \frac{1}{\sqrt{2\pi\sigma\tau_0}} \exp\left[-\frac{\ln^2(\omega/\omega_0)}{2\sigma^2}\right], \quad (5)$$

where τ_0 is a material-dependent parameter, $\omega_0 (=k_B T_0/\hbar)$ is the thermal frequency, and σ is the standard deviation that describes the deviations from ω_0 . Here, we consider a general approach in which the relaxation times are written in a frequency-dependent form such that $\ln(\tau_\ell^{-1}/\tau_0^{-1}) \propto \ln(\omega_\ell/\omega_0)$ [19]. The normalization of Eq. (5) is given through $\int \tau^{-1}(\omega) d\omega = \omega_0 \exp(\sigma^4)/\tau_0$.

In the frame of an adiabatic approximation, we can write that $\dot{u}(\omega, T_2) = u(\omega, T_2)/\tau(\omega)$, where

$$u(\omega, T_2) = \frac{\hbar\omega}{2} \coth\left(\frac{\hbar\omega}{2k_B T_2}\right) \quad (6)$$

is the energy of a harmonic oscillator. Since the tails of the log-normal, when $(\omega/\omega_0) \rightarrow 0$ or ∞ , are negligible, the extreme modes possess such an excessively large relaxation time that they do not contribute to the rate of energy change. Rather, the main influence over the general dynamics, represented by the temporal behavior of the total energy, comes from the shorter time scales of the hierarchy $\tau(\omega)$, that is, for modes around the maximum of the log-normal ($0 < \omega/\omega_0 \lesssim 1$). The log-normal distribution is systematically used to describe the relaxation of

processes consisting of many different elementary subprocesses, as occurs in many cases [21–24].

The hierarchy of relaxation times given through Eq. (5) accounts for dissipation in the system. In fact, $\tau^{-1}(\omega)$ represents the asymptotic of the diffusion coefficient. This circumstance points out the close relation between the interaction forces and dissipation via the fluctuation-dissipation theorem [25]. In addition, the introduction of $\tau^{-1}(\omega)$ leads to a new model for the dielectric permittivity [26],

$$\epsilon(\omega) = \epsilon_\infty + \frac{\epsilon_s - \epsilon_\infty}{1 + i\omega\tau(\omega)}, \quad (7)$$

where ϵ_∞ is the permittivity at the infinite frequency and ϵ_s is the static dielectric constant. Equation (7) corresponds to a generalized Drude relation that accurately incorporates the dissipative effects, in contrast to the plasma model, which does not include dissipation.

Therefore, the power absorbed by the hot material can be written as

$$\dot{Q}_1(\omega) = a_1(\omega, T_1, T_2) e_2(\omega, T_2) \dot{u}(\omega, T_2), \quad (8)$$

and, similarly,

$$\dot{Q}_2(\omega) = a_2(\omega, T_1, T_2) e_1(\omega, T_1) \dot{u}(\omega, T_1), \quad (9)$$

giving the power absorbed by the cold material. Since the temperatures of the objects are different, $\dot{Q}_1(\omega) \neq \dot{Q}_2(\omega)$ and, consequently, the Kirchhoff law establishing the balance between emitted and absorbed power is not applicable.

It was shown in Ref. [7] that the PFA is not consistent with Heisenberg's uncertainty principle. On the contrary, in order to establish a relation between angular frequency and intersurface separation, we assume that Heisenberg's principle applies for position x and momentum p of a photon. Therefore, $\Delta x \Delta p \geq \hbar/2$, and given that the maximum value of Δx is d , one obtains $\Delta p \geq \hbar/(2d)$. In addition, provided the energy $E = p\nu c$, with $\nu < 1$ (ν being the inverse of the refraction index) and where p is implicitly identified with the Minkowski momentum, one gets $\Delta E \geq \hbar\nu c/(2d)$, leading to $\Delta\omega \geq 2\pi\nu c/d \equiv \omega_m$, which establishes a phononlike cutoff frequency [26]. Hence, the total power is given by

$$\mathcal{P}_{i \rightarrow j} = \int_{\omega_m}^{\infty} \dot{Q}_j(\omega) g_j(\omega) d\omega, \quad (10)$$

where $g_j(\omega) = V_j \omega^2 / \pi^2 c^3$ is the density of modes in the material j with volume V_j .

In order to compare our theory with some of the experimental results at hand, hereafter we will consider equal temperatures, $T_1 = T_2 = T$. Inasmuch as power is force times velocity, one is led to infer that the interaction

forces per unit area are given through $F_{i \rightarrow j} = \mathcal{P}_{i \rightarrow j}/c$. Here, we can make progress in the analytical calculations by introducing the change of variable $\omega = 1/s$ in such a way that

$$F_{i \rightarrow j} = \frac{1}{c} \int_0^{\omega_m^{-1}} \dot{Q}_j(\omega(s)) g_j(\omega(s)) \frac{ds}{s^2}. \quad (11)$$

According to the mean value theorem, for very short d (ω_m large) we can approximate the previous integral by the value of the integrand in an intermediate value $\tilde{s} = \chi \omega_m^{-1}$ ($\chi < 1$) times the width of the integration interval ω_m^{-1} , resulting in

$$F_{i \rightarrow j} \approx \frac{\omega_m'^2}{c \omega_m} \dot{Q}_j(\omega'_m) g_j(\omega'_m), \quad (12)$$

with $\omega'_m \equiv \omega(\tilde{s})$. Hence, $\omega'_m = \chi^{-1} \omega_m = 2\pi\epsilon c/d$, where we have introduced the new parameter $\epsilon = \nu/\chi$. Since one assumes an incident homogeneous plane wave on the material, which induces a coupling between waves resulting in a multiple of the characteristic frequency $2\pi/d$, it is expected that $\epsilon > 1$.

For simplicity, let us consider $a_j(\omega, T) = e_j(\omega, T) = 1$. Thus, from Eqs. (12) and (5), one obtains

$$F_{i \rightarrow j} \approx \frac{2^{5/2} \pi^{3/2} \hbar \epsilon^5 V_j}{d^4 \sigma \tau_0'} \exp \left[-\frac{\ln^2(2\pi\epsilon c/\omega_0 d)}{2\sigma^2} \right] \times \coth \left(\frac{\hbar \epsilon c}{2k_B T d} \right), \quad (13)$$

with $\tau_0' = \nu \tau_0$. Unlike Eq. (2), one can notice that Eq. (13) does not diverge as d goes to zero. Additionally, at the limit of large separations, one can perform a Laurent series expansion of $\coth(\cdot)$. By retaining the dominant term, the prefactor in front of the exponential becomes proportional to $k_B T/d^3$. Note that according to our previous discussion on the range of frequencies, the main contribution to the interaction force comes from those modes for which $0 < 2\pi\epsilon c/\omega_0 \lesssim d < \infty$.

Results and discussions.—In order to verify our theory, we compare Eq. (13) with two experimental results. The first of them proves the validity of our approach for both the attractive and the repulsive Casimir forces observed by Munday *et al.* [10]. Regarding the second, we compare Eq. (13) normalized by Eq. (1) to measurements performed by Krause *et al.* [13], extending the limits beyond the PFA.

Atomic force microscopy measurements of Casimir-Lifshitz forces were performed by Munday *et al.* [10] and conducted between a $39.0 \mu\text{m}$ diameter gold sphere with a large plate of silica (repulsive effect) or gold (attractive effect). The gold sphere corresponds to a polystyrene (PS) core coated with a 100 nm thick gold shell and the gold plate corresponds to a silica substrate

coated with 200 nm of gold (for details, see Ref. [10]). The gold nanoshell on the PS sphere can tune the peak of the surface plasmon absorbance band from the visible to the infrared [27], which can be associated with collective effects, e.g., oscillations of the conduction electrons confined in the nanoparticle [28]. The repulsive effects for force measurements were obtained when the sphere-plate setup was enclosed within a bromobenzene-filled cell. As seen in Fig. 1(a), a good agreement is obtained comparing Eq. (13) (black solid lines) with experimental results. For

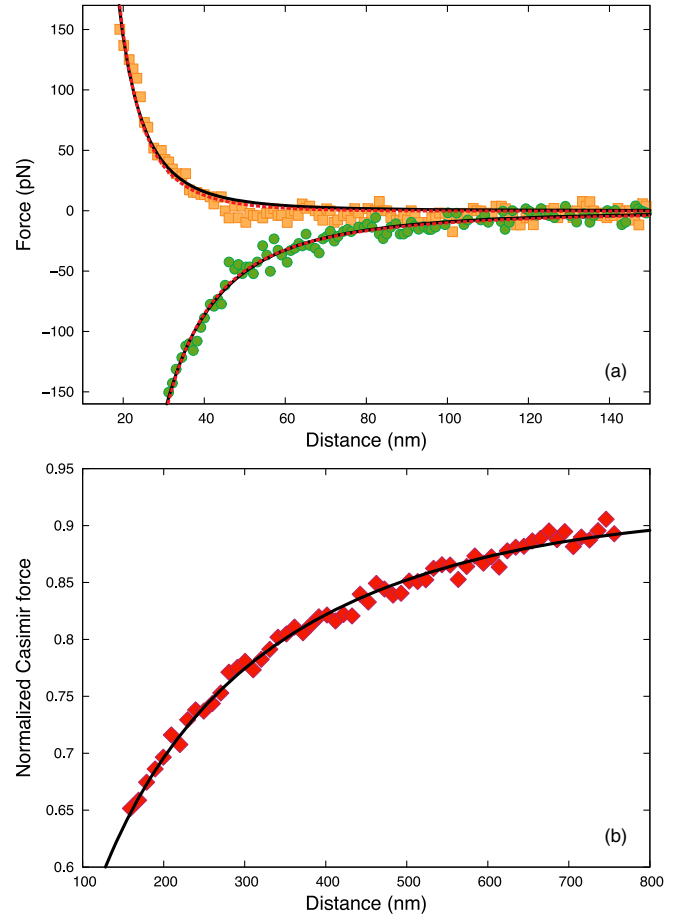


FIG. 1. Casimir-Lifshitz force comparison. (a) Attractive and repulsive Casimir-Lifshitz force between a gold sphere and silica plate versus gap distances using an atomic force microscopy technique. Yellow squares (repulsive) and green circles (attractive) represent data from Munday *et al.* [10] for measurement conducted between a large plate and a $39.8 \mu\text{m}$ diameter sphere. The black solid lines are comparisons with our model, Eq. (13). The red dotted lines are comparisons with the redefined equation from the proximity-force theory with nonstandard values for α and β , Eq. (2). (b) Normalized Casimir-Lifshitz force between a gold sphere and gold plate versus gap distances. The red diamonds represent data from Krause *et al.* [13] using a microelectromechanical torsion oscillator for measurement conducted between a large plate and a $148.2 \mu\text{m}$ radius sphere. The black solid line is the comparison with our approach, Eq. (13) divided by Casimir force assuming that the PFA is valid.

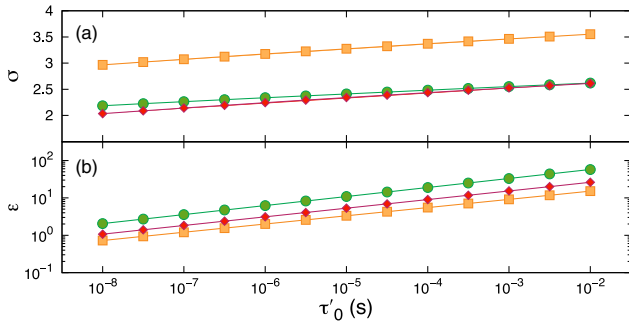


FIG. 2. Fit parameters (a) σ and (b) ϵ vs thermal relaxation times τ'_0 . The parameters have been obtained by considering the thermal frequency, $\omega_0 = k_B T_0 / \hbar \propto 3.836 \times 10^{13} \text{ rad s}^{-1}$. The raw data used for each interaction were the normalized Casimir-Lifshitz force measurements from Krause *et al.* [13] and the repulsive (yellow squares) and the attractive (green circles) Casimir-Lifshitz force measurements from Munday *et al.* [10].

the repulsive (attractive) force fitting we have used $\epsilon = 2.57(8.21)$ and $\sigma = 3.22(2.37)$. The corrected PFA (red dotted lines), Eq. (2), fits experiments with fitting values different from those predicted in the literature (see references contained in Ref. [13]). The repulsive (attractive) behavior displayed in Fig. 1(a) is obtained with $\alpha = 2.82 \times 10^{-2} \pm 0.06 \times 10^{-2} (4.44 \times 10^{-2} \pm 0.05 \times 10^{-2})$ and $\beta = -2.3 \times 10^2 \pm 0.1 \times 10^2 (6.3 \times 10^2 \pm 0.1 \times 10^2)$. Notice that α and β strongly deviate from expected values from the PFA [13].

In Fig. 1(b), we also compare Eq. (13) normalized by Eq. (1) with the measurements of Krause *et al.* [13], taking into account a $148.2 \mu\text{m}$ sphere radius. Their experiments were conducted by using a micromachined torsional oscillator measuring the (normalized) Casimir-Lifshitz force for a gold sphere-plate geometry. For the sphere, a thin layer ($\sim 5 \text{ nm}$) of Cr was deposited and encapsulated by a gold shell of thickness of about 200 nm (for details, see Ref. [13] and references therein). As in the original work of Krause *et al.*, we were not able to adjust the corrected PFA, Eq. (2), to the data. However, the model we propose here does indeed adequately adjust. For this, we have used $\epsilon = 10.23$ and $\sigma = 2.46$.

From the thermal diffusivity, we are able to estimate the thermal relaxation time. Since a particle of radius R and thermal diffusivity D_t requires a characteristic time $\tau'_0 = R^2/D_t$ for the heat to diffuse throughout its volume [29], one obtains $\tau'_0 = 3.12 \times 10^{-6} \text{ s}$ for data from Munday *et al.* [10] and $\tau'_0 = 1.72 \times 10^{-4} \text{ s}$ for data from Krause *et al.* [13]. In addition, we assume that these systems are supposed to be maintained at room temperature and the thermal frequency $\omega_0 \approx 3.836 \times 10^{13} \text{ rad s}^{-1}$.

In such circumstances, we have used the nonlinear least-squares Marquardt-Levenberg algorithm to obtain σ and ϵ as functions of τ'_0 , as depicted in Figs. 2(a) and 2(b), respectively. The best fitting for each τ'_0 value exhibits a

logarithmic behavior for σ , at 94% confidence level, and power law behavior for ϵ , at 97% confidence level. As expected, notice that $\epsilon > 1$, demonstrating the effects of plane waves on surface plasmon excitation and their relation with the thermal relaxation process.

In summary, we have presented a model that properly describes both the attractive and the repulsive experiments on the measurement of the Casimir-Lifshitz forces [10,13]. Equation (13) forms an important link between thermokinetics and relaxation dynamics of the vibrational modes, going beyond the PFA. Our analysis has accurately captured the Casimir-Lifshitz force behavior for a sphere-plate geometry. Here, it must be stressed that the geometric approximation inherent to the PFA is not supplanted by the kinetic description, but rather the values assigned to the parameters of the hierarchy of relaxation times correspond to the sphere-plate geometry. Further study of other geometrical configurations would be of interest. In addition, as pointed out previously, at the limit of large separation the force given by Eq. (13) behaves as $k_B T/d^3$, while at zero temperature we obtain $(1/d^4)$, which in both cases agrees with the conventional Casimir-Lifshitz theory. Moreover, our results have revealed that a distinctive characteristic frequency $\propto 1/d$ can be associated with the surface plasmon resonance. Our model sheds light on the possibility to describe Casimir-Lifshitz forces between a sphere and a large plate, avoiding underestimation of α and β [14].

This work was supported by the CNPq of the Brazilian Government and MICINN of the Spanish Government under Grant No. FIS2008-04386. J. M. R. acknowledges financial support from Generalitat de Catalunya under program ICREA Academia.

-
- [1] H. B. G. Casimir, Proc. K. Ned. Akad. Wet. **51**, 793 (1948).
 - [2] E. M. Lifshitz, ZhETF **29**, 94 (1956) [Sov. Phys. JETP **2**, 73 (1956)].
 - [3] S. K. Lamoreaux, Phys. Rev. Lett. **78**, 5 (1997).
 - [4] S. K. Lamoreaux, Rep. Prog. Phys. **68**, 201 (2005).
 - [5] B. Derjaguin, Kolloid Z. **69**, 155 (1934).
 - [6] J. Blocki, J. Randrup, W. J. Swiatecki, and C. F. Tsang, Ann. Phys. (N.Y.) **105**, 427 (1977).
 - [7] H. Gies and K. Klingmüller, Phys. Rev. Lett. **96**, 220401 (2006).
 - [8] A. Lambrecht, Phys. World **15**, 29 (2002).
 - [9] E. Buks and M. L. Roukes, Phys. Rev. B **63**, 033402 (2001).
 - [10] J. N. Munday, F. Capasso, and V. A. Parsegian, Nature (London) **457**, 170 (2009).
 - [11] G. L. Klimchitskaya, U. Mohideen, and V. M. Mostepanenko, Rev. Mod. Phys. **81**, 1827 (2009).
 - [12] A. W. Rodriguez, F. Capasso, and S. G. Johnson, Nat. Photonics **5**, 211 (2011).
 - [13] D. E. Krause, R. S. Decca, D. López, and E. Fischbach, Phys. Rev. Lett. **98**, 050403 (2007).

- [14] G. Bimonte, T. Emig, and M. Kardar, *Appl. Phys. Lett.* **100**, 074110 (2012).
- [15] A. Canaguier-Durand, P. A. Maia Neto, A. Lambrecht, and S. Reynaud, *Phys. Rev. Lett.* **104**, 040403 (2010).
- [16] *Casimir Physics*, edited by D. Dalvit, P. Milonni, D. Roberts, and F. da Rosa, The Lecture Notes in Physics Vol. 384 (Springer-Verlag, Berlin, 2011).
- [17] A. Scardicchio and R. L. Jaffe, *Nucl. Phys.* **B743**, 249 (2006).
- [18] G. Bimonte, T. Emig, R. L. Jaffe, and M. Kardar, *Europhys. Lett.* **97**, 50001 (2012).
- [19] *Thermal Nanosystems and Nanomaterials*, edited by S. Volz, Topics in Applied Physics Vol. 118 (Springer-Verlag, Berlin, 2009).
- [20] H. Mouri, *Phys. Rev. E* **88**, 042124 (2013).
- [21] E. W. Montroll and M. F. Shlesinger, *Proc. Natl. Acad. Sci. U.S.A.* **79**, 3380 (1982).
- [22] W. A. Yager, *J. Appl. Phys.* **7**, 434 (1936).
- [23] Y. V. Denisov and A. P. Rylev, *Pis'ma Zh. Eksp. Teor. Fiz.* **52**, 1017 (1990) [*JETP Lett.* **52**, 411 (1990)].
- [24] E. Limpert, W. A. Stahel, and M. Abbt, *BioScience* **51**, 341 (2001).
- [25] R. Kubo, M. Toda, and N. Hashitsume, *Statistical Physics II: Nonequilibrium Statistical Mechanics*, Springer Series in Solid-State Sciences Vol. 31 (Springer-Verlag, Berlin, 1978), pp. 1–281.
- [26] A. Pérez-Madrid, L. C. Lapas, and J. M. Rubí, *PLoS One* **8**, e58770 (2013).
- [27] K.-T. Yong, Y. Sahoo, M. T. Swihart, and P. N. Prasad, *Colloids Surf. A* **290**, 89 (2006).
- [28] R. D. Averitt, S. L. Westcott, and N. J. Halas, *J. Opt. Soc. Am. B* **16**, 1824 (1999).
- [29] J.-J. Greffet, Laws of macroscopic heat transfer and their limits, in *Microscale and Nanoscale Heat Transfer* (Springer-Verlag, Berlin, 2007), Vol. 107, pp. 1–13.